Published in final edited form as:
Ann Biomed Eng. 2013 June ; 41(6): . doi:10.1007/s10439-013-0788-4.

Resting EEG Discrimination of Early Stage Alzheimer's Disease from Normal Aging Using Inter-Channel Coherence Network Graphs

Joseph McBride[a], **Xiaopeng Zhao**[a,b], **Nancy Munro**[c], **Charles Smith**[d,f], **Gregory Jicha**[d,f], and **Yang Jiang**[e,f]

[a]Department of Mechanical, Aerospace, and Biomedical Engineering, University of Tennessee, Knoxville, Knoxville, TN 37996

[b]National Institute for Mathematical and Biological Synthesis, University of Tennessee, Knoxville, Knoxville, TN 37996

[c]Oak Ridge National Laboratory, retired, Oak Ridge, TN 37831-6418

[d]Department of Neurology, University of Kentucky, Lexington, KY 40356

[e]Department of Behavioral Science, University of Kentucky, Lexington, KY 40356

[f]Sanders-Brown Center on Aging, University of Kentucky, Lexington, KY 40356

Abstract

Amnestic mild cognitive impairment (MCI) is a degenerative neurological disorder at the early stage of Alzheimer's disease (AD). This work is a pilot study aimed at developing a simple scalp-EEG-based method for screening and monitoring MCI and AD. Specifically, the use of graphical analysis of inter-channel coherence of resting EEG for the detection of MCI and AD at early stages is explored. Resting EEG records from 48 age-matched subjects (mean age 75.7 years)—15 normal controls (NC), 16 with early stage MCI, and 17 with early stage AD—are examined. Network graphs are constructed using pairwise inter-channel coherence measures for delta-theta, alpha, beta, and gamma band frequencies. Network features are computed and used in a support vector machine model to discriminate among the three groups. Leave-one-out cross-validation discrimination accuracies of 93.6% for MCI vs. NC ($p<0.0003$), 93.8% for AD vs. NC ($p<0.0003$), and 97.0% for MCI vs. AD ($p<0.0003$) are achieved. These results suggest the potential for graphical analysis of resting EEG inter-channel coherence as an efficacious method for noninvasive screening for MCI and early AD.

Keywords

EEG-based diagnosis; early Alzheimer's disease; mild cognitive impairment; coherence; graphical analysis

INTRODUCTION

Amnestic mild cognitive impairment (MCI) is a neurological disorder which accompanies early-stage Alzheimer's disease (AD) in the majority of cases that are followed longitudinally to clinically diagnosed dementia[15,16]. Currently MCI is detected based on

Please send correspondence to: X. Zhao, Ph.D., 313 Perkins Hall, University of Tennessee, Knoxville, Knoxville, TN 37996-2010, Phone: (865) 974-7682, Fax: (865) 974-6372, xzhao9@utk.edu.

self/family-reported behavioral histories and some more objective measures including written and task-based neurological and neuropsychological assessments, but typically not in the primary care setting[25]. By the time a primary care provider detects significant changes, the patient has often progressed to AD. Currently, one of the more definitive means for diagnosing AD is determination of cerebrospinal fluid (CSF) biomarker proteins; this, however, requires patients to undergo a lumber puncture, a painful and potentially dangerous procedure[1,26]. Additionally, more advanced imaging techniques, including computed tomography (CT), magnetic resonance imaging (MRI) and positron emission tomography (PET) scans, may also be performed. Unfortunately, the expense and lack of access to these diagnostic methods in a primary care setting often deters physicians from ordering them routinely. A recent area of research has explored the development of more convenient and noninvasive means for screening for MCI/AD, including the use of scalp electroencephalography (EEG).

Symptoms of dementia are caused by the death of cortical neurons and cholinergic deficits (among other concomitants) which subsequently cause a loss of local and global neuronal connectivity in the brain[7,13,19,21]. The neurons of the brain constitute an extremely complex structural network responsible for phenomena as abstract as consciousness, emotion, and memory. The organization of neurons in the brain provides the physiological basis for information processing. One means of attempting to quantify the structural and functional organization of the brain is the application of graph theory to electromagnetic measures of physiological brain activity such as functional MRI (fMRI) and EEG.

A graphical network's complexity is typically quantified in terms of statistical randomness and regularity among the network's connections[24]. More recent research has demonstrated that the behavior in complex systems (e.g., the human brain) is shaped by the interactions among the network's constituent elements[5]. Brain networks characteristically demonstrate small-world behavior, or clustering[3,9,17,22,23]. Small-world behavior is the occurrence of highly connected clusters of nodes within a larger network. Brain network connections are known to exist on a microscopic level (neurons) and macroscopic level (inter-regional)[5]. Connections between nodes in a graphical network are typically based on some measure of association between nodes. In the brain, the probability of connections existing between nodes in a network representing structural (neuronal) connectivity is highly correlated with the physical spatial distance between nodes[2,6,11]. For network models of functional connectivity, however, the relationship between functional connectivity and physical spatial distance is more weakly correlated, as nonadjacent regions of the brain may function in concert during certain cross-modal tasks. For example, previous investigations of network graphs derived from fMRI measures have revealed that functionally-and anatomically-related brain regions are more densely connected, suggesting that connection density between nodes is likely a function of both physical spatial distance (anatomical relationships) and level of functional codependence[8,14,18].

In analyzing changes in human brain organization in dementia, fMRI and EEG networks have clear differences. fMRI has the best spatial resolution (on the order of millimeters) but poor temporal resolution (on the order of seconds) which restricts measurable bandwidth. fMRI measures response-related hemodynamics rather than directly measuring neuronal activity. The nodes used in fMRI networks are anatomically localized regions or voxels in fMRI images. Such nodes allow for various physiological measures for which the association of time series data may be capable of assessing both structural and functional connectivity[5]. Conversely, scalp EEG has poor spatial resolution, but is capable of larger bandwidths (e.g., 0–500 Hz). Typically, EEG electrodes are used as nodes in network graphs. EEG is not well-suited to the study of structural organization in the brain. EEG also has its own inherent limitations as a method of quantifying functional brain organization due

to diffusion of voltage in EEG—namely, different electrodes at different locations across the scalp may be affected by similar sources. For example, eye blink and other muscular artifacts are commonly found in electrodes' signals regardless of position on the scalp. Despite these limitations, EEG is still capable of measuring patterns in neuronal electrical activity more directly than fMRI[5].

In this study, network features of EEG inter-channel coherence measures are examined as a means of detecting and differentiating between normal aging, MCI, and AD at early stages. Specifically, network features describing the global and regional uniformity in delta-theta, alpha, beta, and gamma activity during resting state and a simple cognitive task will be explored.

MATERIALS AND METHODS

Participants

The EEG data used in this study were collected in the laboratory of Dr. Yang Jiang of the Behavioral Science Department and Sanders-Brown Center on Aging at the University of Kentucky (UK) College of Medicine. Participants between the ages of 60 and 90 years were recruited from a study cohort of cognitively normal older adults identified by the Alzheimer's Disease Center (ADC) of the UK College of Medicine. The patients with mild cognitive impairments were recruited from the Memory Disorders Clinic of the ADC. The normal older participants are screened regularly and when screenings indicate possible cognitive decline they are referred to the ADC's Research Memory Disorders Clinic. The MCI and AD participants were diagnosed and recruited by cognitive neurologists Drs. C. Smith and G. Jicha at the UK ADC Clinical Core and from its Research Memory Disorders Clinic. A list of the neurological assessments used to make the diagnoses is provided in Table 1. The MCI and early AD participants' EEG data were recorded as soon as possible after diagnoses were made, most often on the same day. All participants were required to have no medical history of brain tumors or other abnormal brain conditions. No participants were to have the ApoE4 allele for Alzheimer's risk or to be on any psychoactive medication other than antidepressants. Participants were well-matched with regards to age, with normal controls, MCI, and AD participants having mean ages of 75.7 years (SD 5.5 years), 74.6 years (SD 9.0 years), and 76.7 years (SD 5.2 years). NC and AD participants were also well-matched in regards to gender, with NC and AD participants being comprised of 60% females. MCI participants were only 25% female. Difference in MCI gender was likely due to recruiting and does not reflect population trends.

EEG Protocols

Participants were connected to 64- or 32-channel EEG caps using a Neuroscan II system (10–20 montage). In either case, only the 32 common channels were recorded. EEG data were recorded under a protocol using three different non-memory-task conditions. These included (1) resting with eyes open for 5 minutes, (2) resting with eyes closed while counting backwards by ones for 10 minutes while tapping a finger, and (3) resting with eyes closed for 10 minutes, followed by another 5 minutes of eyes open while resting. The EEG recording was performed without interruption at the same appointment for each subject. EEG data were acquired at 500 Hz. The 32 EEG channels included 2 ocular channels which were used to determine the dominant eye blink frequency. Notch filters were used to remove dominant eye blink frequencies and to remove 60 Hz frequencies, which may have been amplified by background electronic devices. A simple 2^{nd} order Butterworth filter was used to attenuate frequencies greater than 200 Hz. In addition, analysis of EEG data examined only frequency components less than 40 Hz.

Coherence Measures

Inter-channel coherence was computed for all pairwise combinations of the 30 electrodes (32 channels with 2 ocular channels excluded) for samples of 2 min duration for all 3 conditions using coherence functions in MATLAB™. Magnitude squared coherence (C_{xy}) is defined by Equation (1), where P_{xy} is the cross-power spectral density, P_{xx} and P_{yy} are the auto-power spectral densities of electrodes x and y, respectively, and f is frequency. Coherence was computed using Welch's averaged, modified periodogram method with windows of 2 seconds and 50% overlap. A 50% cosine taper was applied to each window. Choice of window length and tapering window were based on methods for computing other common spectral features of EEG presented by previous researchers[20].

$$C_{xy}=\frac{|P_{xy}(f)|^2}{P_{xx}(f)P_{yy}(f)} \quad (1)$$

Mean coherence values ($\overline{C_{xy}}$) were determined for four physiologically relevant frequency bands: (1) delta-theta (δ, 0—7.5 Hz), (2) alpha (α, 7.5—12.5 Hz), (3) beta (β, 12.5—25 Hz), and gamma (γ, 25—40 Hz). Delta-theta frequencies are associated with sleeping, drowsiness, and daydreaming; alpha and beta bands are associated with being awake and alert; gamma band frequencies are associated with short-term memory and cross-modal tasks. These four mean coherence values were used to determine connections in graphical network representations of inter-channel coherence.

Inter-Channel Coherence Networks

A graphical network representation of inter-channel coherence was constructed for each of the four frequency bands. Nodes in each network were defined as the EEG electrode channels. Mean coherence values for corresponding frequencies were used as measures of associations between nodes. Weights were assigned to all pairwise connections in the networks and were equal to the complement of the mean coherence values. For example, for a mean coherence value between channels x and y among α band frequencies ($\overline{C_{xy}^{\alpha}}$), the corresponding weight $w_{xy}^{\alpha}=1-\overline{C_{xy}^{\alpha}}$. Thus, the lower the weight, the stronger the coherence of the given frequency activity between two electrodes. Thresholds of 0.567, 0.481, 0.402, and 0.303 were applied to weights of the δ, α, β, and γ band networks, respectively. Connections with weights *below* these thresholds were included while connections with weights greater than these thresholds were severed. The choice of thresholds was based on the observation that 75% of weights among all subjects were above the thresholds.

Network Features

Sixteen features were computed for each of the 4 network graphs corresponding to the 4 frequency bands for a total of 64 features; see Table 2 for a list of network features computed. The set of features includes four global network features and 12 regional network features. The first global network feature is connection density (D). Connection density is equal to the percentage of possible connections which passed the threshold significance criterion and are actually present in the network (existing connections). Other global features included statistical features summarizing the distribution of existing connections' weights. Specifically, the maximum likelihood estimates of the scale (A) and shape (B) parameters for a Weibull distribution fit of the weights' probability density function (PDF) were determined. These parameters allow for analysis of the general trends in the strength of coherence between significant (existing) connections.

An additional global network feature computed included the mean number of nodes ($\bar{N}$) in the shortest existing pathways between nodes. Given the severing of connections via the threshold criterion, a pathway does not necessarily exist between any two given nodes. Furthermore, given that the length of a pathway is equal to the sum of the weights of connections in a pathway and that the weights are equal to the complement of the coherence between nodes, the shortest pathway between two nodes is also the pathway of strongest coherence between constituent nodes in the pathway. Because coherence is a measure of the correlated general trends of two time series at a given frequency, it is also a measure of mutual information between frequency activities of the two time series. Viewed in this context, the shortest pathway between two nodes is both the pathway of strongest coherence and the pathway of greatest mutual information in the specific frequency band for the given start and end nodes. The mean number of nodes in the shortest existing pathways is therefore an average measure of the interdependence of mutual information among connected nodes in the given frequency range.

In addition to the four global network features described above, hub order and clustering coefficients were also examined on a regional basis. Hub order (H) for a given node is defined as the number of existing shortest pathways which include the node, excluding pathways which begin or end at the given node. Clustering coefficient (K) for a given node is a measure of the connection density among local nodes. In this study, clustering coefficient for a given node is defined as the number of direct connections between the directly connected nodes divided by the number of possible connections between directly connected nodes. Both hub order and clustering coefficients were averaged over six scalp regions: central (C), frontal (F), left temporal (L), parietal (P), occipital (O), and right temporal (R). See Fig. 1 for a diagram of the region boundaries.

The implications of the values of the chosen network features regarding the EEG electrical activity are summarized in Table 3, where the superscript (f) denotes the frequency band and the subscript (r) denotes the region (if applicable). A low connection density (D) value is indicative of low global coherence and implies diverse sources for the recorded electrical activity in the given frequency band. Conversely, high D is indicative of high global coherence and greater uniformity in the electrical activity in the given frequency band. The weight's PDF scale parameter (A) has the opposite relationship, with a low value implying high coherence and a high value implying low coherence. The PDF shape parameter (B) is indicative of the variation in coherence values, with a low value suggesting low variation and a high value suggesting high variation. The mean number of nodes in the shortest existing pathways ($\bar{N}$), as mentioned previously, serves as a measure of the interdependence of coherence values, with a larger mean number of nodes indicating lower interdependence. Generally, low interdependence in coherence values can be interpreted as implying low uniformity in electrical activity in the given frequency band. Regional mean hub orders ($\overline{H}_r^f$) also indicate interdependence of coherence, but on a regional rather than global scale. These values can be interpreted as indicating the relative interdependence of the given region's coherence with the other regions. Thus, low $\overline{H}_r^f$ could imply low global uniformity in electrical activity or a possible localized source of electrical activity in the given frequency band near or within the specific region. High $\overline{H}_r^f$ is indicative of greater global uniformity in the given frequency band activity. Finally, regional mean clustering coefficients ($\overline{K}_r^f$) serve as indicators of intraregional coherence, with high values suggesting the possibility of a localized source for given frequency activity.

Feature Selection

The three groups of subjects (NC, MCI, and AD) provided three binary discrimination problems: (1) MCI vs. NC, (2) AD vs. NC, and (3) MCI vs. AD. Sixteen network features were computed for four network graphs based on mean inter-channel coherence for δ, α, β, and γ frequency bands. Thus, a total of 64 features were computed for each subject for each protocol condition. Feature selection was performed in order to assess the contribution of individual features to discrimination performance for each binary discrimination problem and each protocol condition. Feature selection was performed as follows. For each discrimination problem and each condition, combinations of up to 8 of the 64 features were tested using support vector machine (SVM) functions in MATLAB™. Quadratic kernel functions were used in all discriminations and the cost coefficient was held constant at unity. To help avoid over fitting, *nested* leave-one-out cross-validation loops were used to suggest and test different combinations of features. The inner loop was used to generate a list of suggested combinations of features using a forward, supervised, high-score feature selection method where combinations were scored using leave-one-out cross-validation accuracy of SVM model predictions based on a smaller, randomized, subset of records[4]. The outer loop determined the leave-one-out cross-validation accuracy of the combinations of features suggested by the inner loop for all available records. The contribution of individual features was then assessed based on how often they appeared in the best 200 performing combinations tested in the outer loop simulations. Ultimately, the six features which appeared most often were then tested in combination.

Statistical Significance

The statistical significance of results obtained using the six selected features chosen via feature selection was assessed using Monte Carlo permutation testing. Specifically, a random sample of 10,000 permutations of shuffled labels was used to estimate a 95% confidence interval for the probability that the leave-one-out cross-validation accuracies obtained were due to chance. The p-values presented were determined using this method.

RESULTS

A summary of the feature selection results is presented in graphical form in Fig. 2, where a color scale is used to indicate the inclusion of given features in the 200 best performing combinations. For example, 100% would indicate that a given feature was included in all of the 200 best performing combinations; 50% indicates inclusion in half of the 200 best performing combinations; etc. As can be seen in Fig. 2, for most binary classification problems and conditions, a few features are clearly highlighted as being highly discriminatory (highly inclusive). One notable exception is the discrimination of MCI vs. NC subjects while counting backwards with eyes closed. As seen in Fig. 2, no set of features is capable of clearly distinguishing the two groups' EEG frequency activity during the given task. Statistical analyses reveal that this failure is due to high variability among feature values within each group, suggesting that the task of counting backwards with eyes closed may be ill-suited for discriminating between MCI and NC subjects based solely on analysis of EEG frequency characteristics.

For each protocol condition and discrimination problem, the six features with the highest inclusivity among feature selection results were selected for further analyses. Firstly, all six features were tested in combination. The results are summarized in Table 4. 95% confidence intervals for corresponding p-values of the resulting leave-one-out cross-validation accuracies were assessed using Monte Carlo permutation testing.

Additionally, two-sample Student's t-distribution tests (unequal variance) were performed on group means of individual features in order to determine whether differences between the given samples were great enough to statistically infer differences in the groups' populations (90% confidence). Features for which such an inference could be made are indicated with † in Table 4. Given the small sample sizes, such inference required large differences between group means and small variation within groups. It should be noted that such tests are dependent on the assumption of representative samples.

Finally, the potential implications of differences in EEG electrical activity between groups were assessed for each feature for which differences in population means could be inferred with statistical significance. These observations are summarized in Table 4.

When resting with eyes open, MCI subjects demonstrated greater interdependence of α activity in the central region with other regions, greater interdependence of β activity of the frontal region with other regions, and greater localization of β activity in the occipital region compared to normal controls. These observations suggest overall greater uniformity in α activity and greater localization in β activity for MCI subjects compared to NC subjects. The eyes open, resting condition also demonstrated the greatest accuracy in MCI vs. NC discrimination, with a leave-one-out cross-validation accuracy of 93.6% ($p<0.0003$) using six selected features. Results for MCI vs. NC discrimination while counting backwards with eyes closed were inconclusive, with feature selection failing to suggest likely discriminating features among those tested. While resting with eyes closed, MCI subjects as a whole demonstrated higher mean coherence in α activity and greater localization of γ activity in the frontal region. A leave-one-out cross-validation accuracy of 87.1% ($p<0.0012$) was achieved during the eyes closed, resting condition using six selected features.

A leave-one-out cross-validation accuracy of 81.3% ($p<0.0042$) was achieved for AD vs. NC discrimination during the eyes open, resting condition. Group differences in selected features indicated greater interdependence of α activity of the frontal region with other regions and higher mean coherence in γ activity for AD subjects. Leave-one-out cross-validation accuracies of 93.8% ($p<0.0003$) and 90.6% ($p<0.0003$) were achieved using six selected features for the counting with eyes closed and resting with eyes closed conditions, respectively. Lower global uniformity of δ activity and lower coherence of β activity in the occipital region was observed for the AD subjects during the counting backward condition. When resting with eyes closed, AD subjects clearly demonstrated greater localization of δ activity in the left temporal region and significantly higher variability in γ activity.

The highest discrimination accuracy for MCI vs. AD was observed during the eyes open, resting condition, with a leave-one-out cross-validation accuracy of 97.0% ($p<0.0003$) using six selected features. Statistical analyses of the selected features indicate greater uniformity in δ activity and lower uniformity in α and γ activity in AD subjects compared to MCI subjects. AD subjects also demonstrated greater localization of γ activity in the central region. A leave-one-out cross-validation accuracy of 87.9% ($p<0.0008$) was achieved for the counting backward task using six selected features. Those features point to lower uniformity in α and γ activity and greater uniformity in β activity in AD subjects compared to MCI subjects. Gamma activity features also appear to have greater discriminatory power for the resting with eyes closed condition. A leave-one-out cross-validation accuracy of 87.9% ($p<0.0007$) was also achieved for the resting, eyes closed condition using six selected features.

DISCUSSION

In this study, EEG of *resting state* conditions and a *simple* cognitive task are explored as likely biomarkers for discriminating NC, MCI and AD groups. Resting state protocols and simple cognitive tasks (e.g., counting backwards) eliminate the need for a memory task. Resting states, in particular, do not attempt to elicit specific cognitive responses, thereby making the analysis more robust in regards to patients' states of mind. Interestingly, while the best discrimination between AD and NC subjects was achieved during the counting backward condition, the best results in discriminating MCI from NC and AD subjects was achieved during the eyes open, resting condition, suggesting that cognitively taxing tasks may indeed be unnecessary for eliciting detectable differences in EEG activity for MCI diagnosis.

Previous studies have explored various EEG features for the discrimination of MCI/AD from normal individuals. Several of these researchers have observed that features which appear to discriminate AD from NC well, do not necessarily perform well when applied to MCI subjects[10,12,20]. Often, MCI individuals appear to be spread across boundaries which otherwise clearly discriminate AD from normal subjects. These difficulties are likely due to the nature of MCI diagnoses. By definition, neurological symptoms caused by amnestic MCI do not significantly interfere with normal daily activities. In contrast, when patients are diagnosed with AD, their symptoms have generally progressed significantly. Thus, the diagnosis of MCI constitutes a gray area between normal, age-related cognitive decline (NC) and AD. The high accuracy achieved here in discriminating between MCI and AD on the basis of γ activity is encouraging as there is great interest in being able to detect cognitive decline which may be associated with AD at the earliest stages. It is also worth noting that a different set of features may be required for discriminating between NC, MCI, and AD as features rarely appear to function as a sliding scale with NC at one end, AD at the other, and MCI in the middle.

Previous studies have also demonstrated the applicability of synchronization, coherence, and other association measures between scalp EEG electrodes in the discrimination of normal individuals and those with dementia. Typically, researchers have attempted to identify individual local association measures (e.g., coherence between two specific channels at a specific frequency) or a few globally-averaged association measures which appear to demonstrate significant robustness in discriminating normal individuals from those with dementia. Unfortunately, dementia can cause different neurological changes in different individuals—especially in the case of more enigmatic diagnoses such as MCI. Such differences may lead to the failure in the generalization of local or globally-averaged association measures to other data sets.

This study presents a method for analyzing coherence measures between EEG electrodes via graphical analysis. The success of SVM discrimination between binary groupings of the three groups of EEG records (NC, MCI, and AD) are the result of differences in uniformity of electrical activity in specific frequency bands in resting states and during a simple cognitive task. Specifically, MCI subjects demonstrated greater uniformity in α and β activity than NC subjects when resting with eyes open. AD subjects also demonstrated greater uniformity in α and γ activity when resting with eyes open. When counting backwards, differences between MCI and NC subjects were inconclusive; however, AD subjects demonstrated lower uniformity of δ and β activity in the parietal and occipital regions, respectively, compared to NC subjects. When resting with eyes closed, MCI subjects demonstrated greater uniformity in α activity and greater localization in γ activity in the frontal region while AD subjects demonstrated greater localization of δ activity in the left temporal region and higher variation in γ coherence. Differences between MCI and AD

subjects were primarily observed with regards to γ activity in all three conditions. It is possible that these differences may be the results of characteristic changes in brain network functional organization (e.g., compensatory mechanisms) as a result of neurological degeneration.

The results of this work suggest the possible potential for the use of network graphs representing scalp electrical activity relationships as a means for objectively discriminating between normal, MCI, and AD patients. Results suggest that a simple discrimination model utilizing SVM and the network features presented here may be a viable basis for future development of a diagnostic screening tool for MCI and early AD with applicability in the primary care setting. Such a rapid, simple, and cost-effective tool could also prove useful in the drug discovery process. One limitation of this study is the small number of participants. Future work will increase the sample size to test the robustness and generality of the results here.

Acknowledgments

We thank A. Lawson, J. Howe, E. Walsh, J. Lianekhammy, S. Kaiser, C. Black, K. Tran, and L. Broster at UK for their assistance in data acquisition and database management. Research was sponsored in part by the Laboratory Directed Research and Development Program of Oak Ridge National Laboratory, managed by UT-Battelle, LLC, for the US Department of Energy under Contract No. DE-AC05-00OR22725, and in part by the NSF under grant number CMMI-0845753; DOE OR-22725 to NM, NIH AG00986 to YJ, NCRRUL1RR033173 to UK CTS, P30AG028383 to UK Sanders-Brown Center on Aging.

REFERENCES

1. Anoop A, Singh PK, Jacob RS, Maji SK. CSF biomarkers for Alzheimer's disease diagnosis. Int. J. Alzheimer Dis. 2010; 2010:1–12.
2. Averbeck BB, Seo M. The statistical neuroanatomy of frontal networks in the macaque. PLoSComput. Biol. 2008; 4:e1000050.
3. Bassett DS, Bullmore ET. Small-world brain networks. Neuroscientist. 2006; 12:512–523. [PubMed: 17079517]
4. Bishop, CM. Neural Networks for Pattern Recognition. New York, NY: Oxford University Press, Inc.; 2008. Pre-processing and feature extraction; p. 295-329.
5. Bullmore E, Sporns O. Complex brain networks: theoretical analysis of structural and functional systems. Nat. Rev. Neurosci. 2009; 10:186–198. [PubMed: 19190637]
6. Braitenberg, V.; Schüz, A. Cortex: Statistics and Geometry of Neuronal Connectivity 2nd ed., reviewed by L. Gary. Berlin: Springer; 1998. 249 p.
7. Brenner RP, Ulrich RF, Spiker DG, Sclabassi RJ, Reynolds CF III, Marin RS, Boller F. Computerized EEG spectral analysis in elderly normal, demented and depressed subjects. Electroencephalogr. Clin. Neurophysiol. 1986; 64:483–492. [PubMed: 2430770]
8. Farrarini L, Veer IM, Baerends E, van Tol MJ, Renken RJ, van der Wee NJ, Veltman DJ, Aleman A, Zitman FG, Penninx BW, van Buchem MA, Reiber JH, Rombouts SA, Miles J. Hierarchical functional modularity in the resting-state human brain. Hum. Brain Mapp. 2009; 30:2220–2231. [PubMed: 18830955]
9. Girvan M, Newman MEJ. Community structure in social and biological networks. Proc. Natl. Acad. Sci. USA. 2002; 99:7821–7826. [PubMed: 12060727]
10. He, B. Neural Engineering. New York, NY: Kulwer Academic/Plenum Publishers; 2005. Neural Signal Processing; p. 193-221.
11. Hellwig BA. A quantitative analysis of the local connectivity between pyramidal neurons in layers 2/3 of the rat visual cortex. Biol. Cybern. 2000; 82:111–121. [PubMed: 10664098]
12. Jelic V, Johansson SE, Almkvist O, Shigeta M, Julin P, Nordberg A, Winblad B, Wahlund LO. Quantitative electroencephalography in mild cognitive impairment: longitudinal changes and possible prediction of Alzheimer's disease. Neurobiol. Aging. 2000; 21:533–540. [PubMed: 10924766]

13. Jeong J. EEG dynamics in patients with Alzheimer's disease. Clin. Neurophysiol. 2004; 115:1490–1505. [PubMed: 15203050]

14. Meunier D, Archard S, Morcom A, Bullmore E. Age-related changes in modular organization of human brain functional networks. Neuroimage. 2009; 44:715–723. [PubMed: 19027073]

15. Petersen, R. Mild Cognitive Impairment. New York, NY: Oxford Press; 2003. 288 p.

16. Petersen RC, Parisi JE, Dickson DW, Johnson KA, Knopman DS, Boeve BF, Jicha GA, Ivnik RJ, Smith GE, Tangalos EG, Braak H, Kokmen E. Neuropathologic features of amnestic mild cognitive impairment. Arch. Neurol. 2006; 63:665–672. [PubMed: 16682536]

17. Reijneveld JC, Ponten SC, Berendse HW, Stam CJ. The application of graph theoretical analysis to complex networks in the brain. Clin. Neurophysiol. 2007; 118:2317–2331. [PubMed: 17900977]

18. Salvador R, Suckling J, Coleman MR, Pickard JD, Menon D, Bullmore E. Neurophysiological architecture of functional magnetic resonance images of human brain. Cereb. Cortex. 2005; 15:1332–1342. [PubMed: 15635061]

19. Signorino M, Pucci E, Belardinelli N, Nolfe G, Angeleri F. EEG spectral analysis in vascular and Alzheimer's dementia. Electroencephalogr. Clin. Neurophysiol. 1995; 94:313–325.

20. Snaedal J, Johannesson GH, Gudmundsson TE, Gudmundsson S, Pajdak TH, Johnsen K. The use of EEG in Alzheimer's disease, with and without scopolamine-a pilot study. Clin. Neurophysiol. 2010; 121:836–841. [PubMed: 20153691]

21. Soininen H, Partanen J, Laulumaa V, Helkala EL, Laakso M, Riekkinen PJ. Longitudinal EEG spectral analysis in early stage of Alzheimer's disease. Electroencephalogr. Clin. Neurophysiol. 1989; 72:290–297. [PubMed: 2467794]

22. Sporns O, Chialvo DR, Kaiser M, Hilgetag CC. Organization, development and function of complex brain networks. Trends Cogn. Sci. 2004; 8:418–425. [PubMed: 15350243]

23. Stam CJ, Reijneveld JC. Graph theoretical analysis of complex of complex networks in the brain. Nonlin. Biomed. Phys. 2007; 1:3.

24. Tononi G, Sporns O, Edelman GM. A measure for brain complexity: relating functional segregation and integration in the nervous system. Proc. Natl. Acad. Sci. USA. 1994; 91:5033–5037. [PubMed: 8197179]

25. Waldemar G, Dubois B, Emre M, Georges J, McKeith IG, Rossor M, Scheltens P, Tariska P, Winbald B. Recommendations for the diagnosis and management of Alzheimer's disease and other disorders associated with dementia: EFNS guideline. Eur. J. Neurol. 2007; 14:e1–e26. [PubMed: 17222085]

26. Zetterberg H, Mattson N, Blennow K. Cerebrospinal fluid analysis should be considered in patients with cognitive problems. Int. J. Alzheimer Dis. 2010; 2010:1–4.

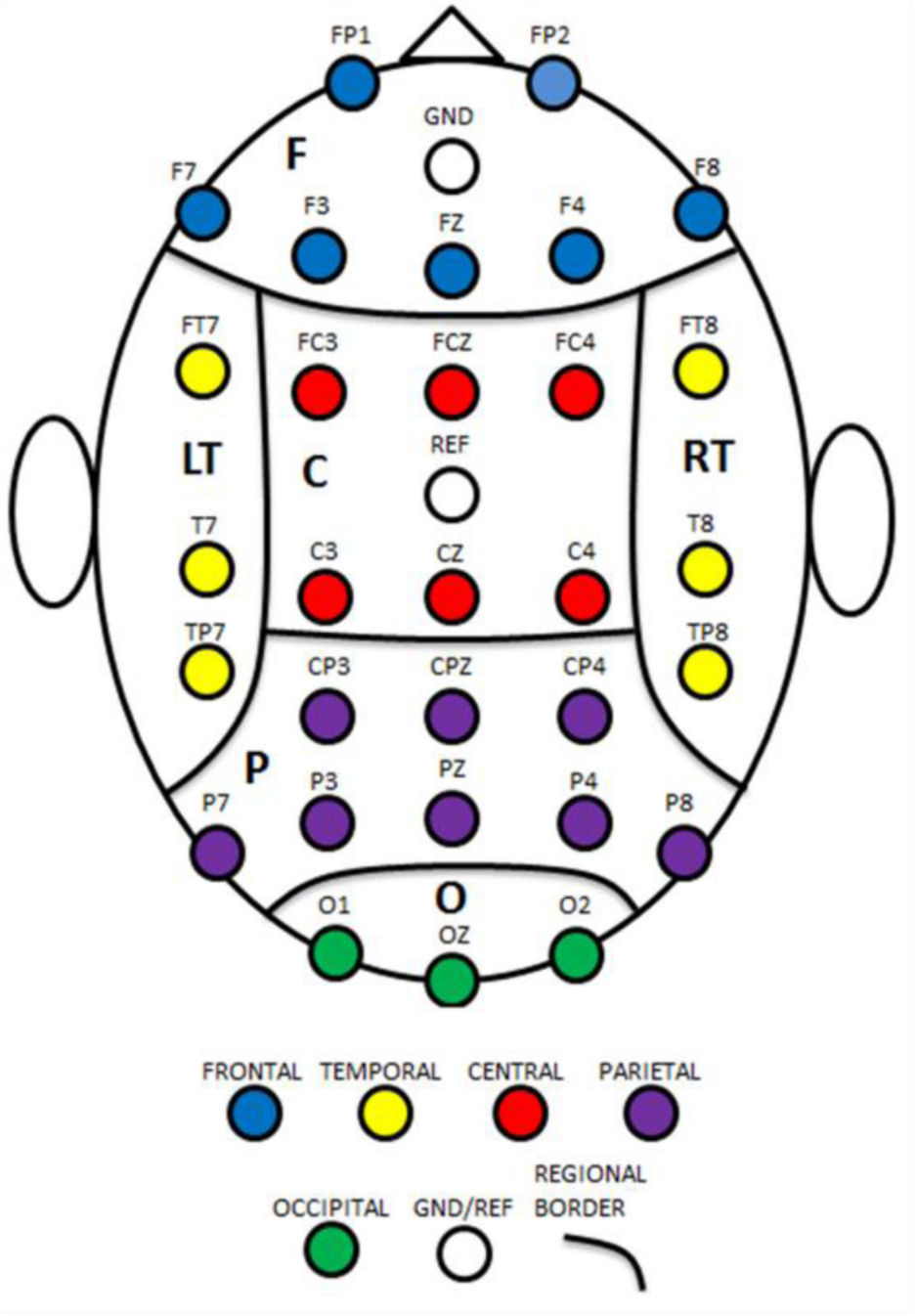

Fig.1.
Boundaries of scalp regions. C = central, F = frontal, L = left temporal, O = occipital, P = parietal, and R = right temporal.

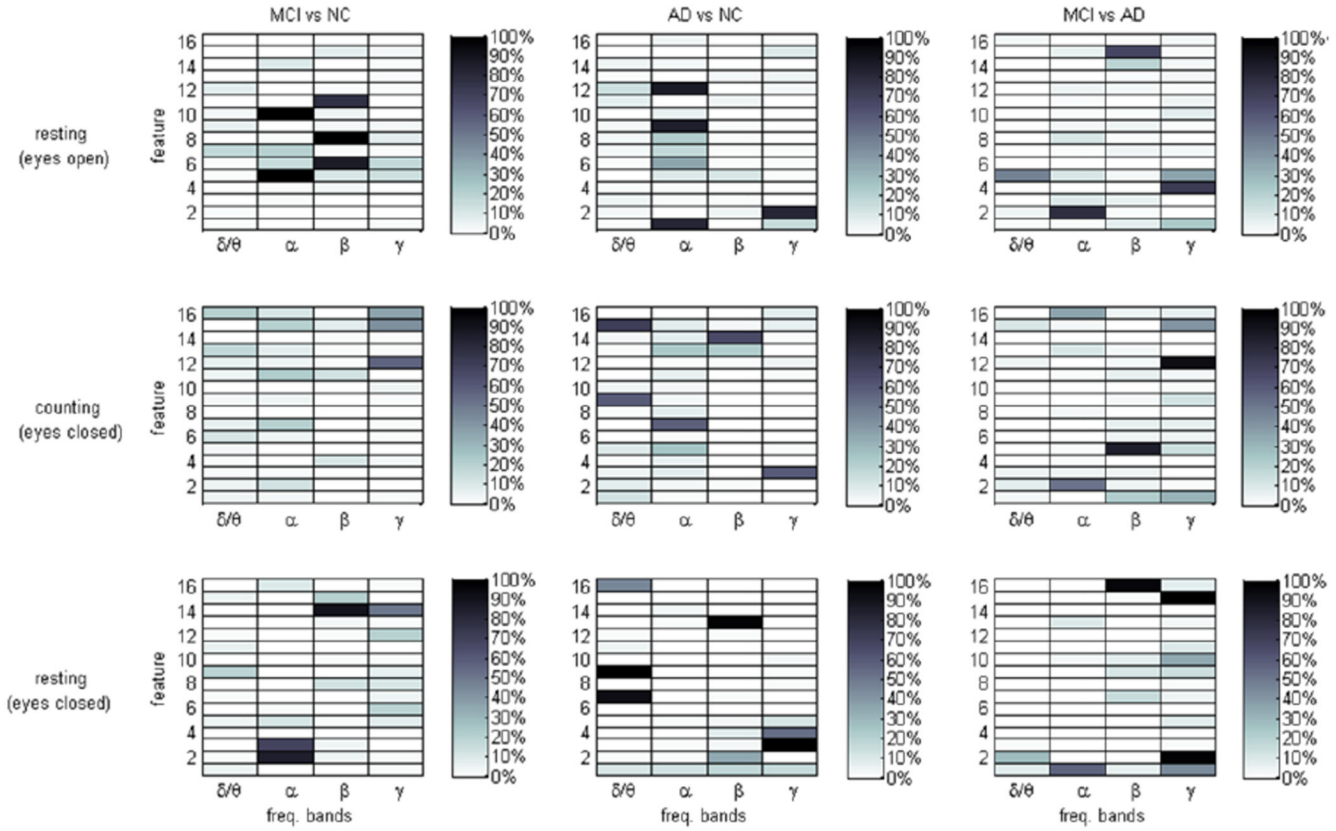

Fig.2.

Feature selection results. Color scale indicates the inclusion of given features in the 200 best performing combinations for the given protocol condition and binary discrimination problem.

Table 1

Cognitive Tests and Other Evaluations Used to Make MCI/AD Diagnoses

General Cognitive Measures	**Baseline Only**
MMSE	National Adult Reading Test
Clinical Dementia Rating (CDR)	
Memory Domain Measures	**Medical Evaluation**
WMS Logical Memory I & II	Physical exam
California Verbal Learning Test	Neurological exam
	Medical history
Attention/Executive Domain Measures	Medications
Trail Making Tests A & B	Nutritional supplements
WAIS-R Digit Span & Digit Symbol	Food Frequency Questionnaire (FFQ)
Language Domain Measures	**Psychiatric Evaluation**
COWAT	Neuropsychiatric Inventory Questionnaire (NPI-Q)
Animal Fluency	Geriatric Depression Scale (GDS)
Vegetable Fluency	
Boston Naming	
	Functional Ability Measures
	Functional Assessment Questionnaire (FAQ)
Visual/Spatial Domain Measures	SF-36
CERAD Figures	ADCS-ADL

Table 2

Network Features

(1)	D	Connection density
(2)	A	Scale parameter of Weibull distribution fit of weights
(3)	B	Shape parameter of Weibull distribution fit of weights
(4)	$\overline{N}$	Mean number of nodes in shortest existing pathways
(5)	$\overline{H}_C$	Mean hub order in central (C) region
(6)	$\overline{H}_F$	Mean hub order in frontal (F) region
(7)	$\overline{H}_L$	Mean hub order in left temporal (L) region
(8)	$\overline{H}_O$	Mean hub order in occipital (O) region
(9)	$\overline{H}_P$	Mean hub order in parietal (P) region
(10)	$\overline{H}_R$	Mean hub order in right temporal (R) region
(11)	$\overline{K}_C$	Mean clustering coefficient in central (C) region
(12)	$\overline{K}_F$	Mean clustering coefficient in frontal (F) region
(13)	$\overline{K}_L$	Mean clustering coefficient in left temporal (L) region
(14)	$\overline{K}_O$	Mean clustering coefficient in occipital (O) region
(15)	$\overline{K}_P$	Mean clustering coefficient in parietal (P) region
(16)	$\overline{K}_R$	Mean clustering coefficient in right temporal (R) region

Table 3

Implications of Network Feature Values for Brain Electrical Activity

Feature	Value	Direct implications for coherence	Implications for *f* band electrical activity
(1) D^f	low	low global coherence	lower uniformity
	high	high global coherence	greater uniformity
(2) A^f	low	high mean coherence	greater uniformity
	high	low mean coherence &/OR high variation in coherence	low uniformity
(3) B^f	low	low variation in coherence	--
	high	high variation in coherence	--
(4) $\bar{N}^f$	low	high interdependence of coherence	greater uniformity
	high	low interdependence of coherence	low uniformity
(5)–(10) $\bar{H}^f_r$	low	coherence in region *r* has low interdependence of with other regions	low uniformity &/OR possible localized source of *f* band activity near/within region *r*
	high	coherence in region *r* has high interdependence of with other regions	greater uniformity
(11)–(16) $\bar{K}^f_r$	low	low coherence within region *r*	--
	high	high coherence within region *r*	possible localized source of *f* band activity near/within region *r*

Table 4

Group Comparisons and Implications of Selected Features

	MCI vs. NC			AD vs. NC			MCI vs. AD		
	Selected Features	**Group Means**	**Implications**	**Selected Features**	**Group Means**	**Implications**	**Selected Features**	**Group Means**	**Implications**
resting (eyes open)	$\overline{H}_C^{\alpha}$	MCI>NC †	greater uniformity in α, β activity; greater localization of β activity in O region	D^{α}	AD<NC	greater uniformity in α, γ activity	$\overline{H}_C^{\delta}$	MCI<AD †	greater uniformity in δ activity in AD; lower uniformity in α, γ activity in AD; greater localization of γ activity in C region in AD
	$\overline{H}_L^{\alpha}$	MCI>NC		$\overline{H}_F^{\alpha}$	AD>NC †		A^{α}	MCI<AD †	
	$\overline{H}_R^{\alpha}$	MCI>NC		$\overline{H}_O^{\alpha}$	AD<NC		$\overline{K}_P^{\beta}$	MCI>AD	
	$\overline{H}_F^{\beta}$	MCI>NC †		$\overline{H}_P^{\alpha}$	AD>NC		$D^{\bar{N}}$	MCI>AD †	
	$\overline{H}_O^{\beta}$	MCI<NC †		$\overline{K}_F^{\alpha}$	AD<NC		$N^{\bar{N}}$	MCI>AD	
	$\overline{K}_C^{\beta}$	MCI>NC		A^{γ}	AD>NC †		$\overline{H}_C^{\gamma}$	MCI>AD †	
	acc. (sens., spec.): 93.6% (93.8%, 93.3%) 95%CI for p-value: (0, 0.0003)			acc. (sens., spec.): 81.3% (82.4%, 80.0%) 95%CI for p-value: (0.0020, 0.0042)			acc. (sens., spec.): 97.0% (93.8%, 100%) 95%CI for p-value: (0, 0.0003)		
counting (eyes closed)	no dominant features available		results inconclusive	$\overline{H}_P^{\delta}$	AD<NC †	lower uniformity in δ activity; lower coherence of δ activity in P region; lower coherence of β activity in O region	A^{α}	MCI<AD †	lower uniformity of α, γ activity in AD; greater uniformity of β activity in AD; greater localization of γ activity in F, P regions in AD
				$\overline{K}_P^{\delta}$	AD<NC †		$\overline{K}_R^{\alpha}$	MCI<AD	
				$\overline{H}_C^{\alpha}$	AD>NC		$\overline{H}_C^{\beta}$	MCI<AD †	
				$\overline{H}_L^{\alpha}$	AD<NC		$D^{\bar{N}}$	MCI>AD †	
				$\overline{K}_O^{\beta}$	AD<NC †		$\overline{K}_F^{\gamma}$	MCI>AD †	
				$B^{\bar{N}}$	AD>NC		$\overline{K}_P^{\gamma}$	MCI>AD †	
				acc. (sens., spec.): 93.8% (100%, 86.7%) 95%CI for p-value: (0, 0.0003)			acc. (sens., spec.): 87.9% (81.3%, 94.1%) 95%CI for p-value: (0.000008, 0.0008)		

	MCI vs. NC			AD vs. NC			MCI vs. AD		
	Selected Features	**Group Means**	**Implications**	**Selected Features**	**Group Means**	**Implications**	**Selected Features**	**Group Means**	**Implications**
resting (eyes closed)	A^{α}	MCI<NC †	greater uniformity in α activity; greater localization of γ activity in F region	$\overline{H}_{L}^{\delta}$	AD<NC †	greater localization of δ activity in L region; higher variation in coherence of γ activity	C^{α}	MCI<AD	lower uniformity in γ activity in AD
	B^{α}	MCI<NC		$\overline{H}_{P}^{\delta}$	AD<NC		$\overline{K}_{R}^{\beta}$	MCI>AD	
	$\overline{K}_{O}^{\beta}$	MCI<NC		$\overline{K}_{R}^{\delta}$	AD<NC		D^{γ}	MCI<AD	
	$\overline{K}_{P}^{\beta}$	MCI<NC		$\overline{K}_{L}^{\beta}$	AD<NC		A^{γ}	MCI<AD †	
	$\overline{K}_{F}^{\gamma}$	MCI>NC †		B^{γ}	AD>NC †		$\overline{H}_{R}^{\gamma}$	MCI>AD †	
	$\overline{K}_{O}^{\gamma}$	MCI>NC		N^{γ}	AD>NC		$\overline{K}_{P}^{\gamma}$	MCI>AD	
	acc. (sens., spec.): 87.1% (93.8%, 80.0%) 95%CI for p-value: (0.0007, 0.0012)			acc. (sens., spec.): 90.6% (94.1%, 86.7%) 95%CI for p-value: (0, 0.0003)			acc. (sens., spec.): 87.9% (81.3%, 94.1%) 95%CI for p-value: (0, 0.0007)		

† p-value <0.10 for two-sample student t-distribution test (unequal variance) of difference in population means